



ORIGINAL ARTICLE

Thermodynamic, chemical and electrochemical investigations of 2-mercapto benzimidazole as corrosion inhibitor for mild steel in hydrochloric acid solutions

M. Benabdellah ^a, A. Tounsi ^b, K.F. Khaled ^{c,d,*}, B. Hammouti ^a

^a Laboratoire de Chimie Appliquée et Environnement, Faculté des Sciences, BP 717, 60 000 Oujda, Morocco

^b Equipe Electrochimie et Environnement, Faculté des Sciences et Techniques, Errachidia, BP 509, Boutalamine Errachidia, Morocco

^c Electrochemistry Research Laboratory, Chemistry Department, Faculty of Education, Ain Shams University, Roxy, Cairo, Egypt

^d Materials and Corrosion Laboratory (MCL), Chemistry Department, Faculty of Science, Taif University, Taif, Saudi Arabia

Received 8 May 2010; accepted 8 June 2010

Available online 18 June 2010

KEYWORDS

Mild steel;
2-Mercaptobenzimidazole;
Acid inhibition;
EIS;
Adsorption;
Thermodynamic parameters

Abstract The inhibiting action of 2-mercapto benzimidazole (2MBI) on mild steel in 1.0 M hydrochloric acid has been investigated at 308 K using weight loss measurements and electrochemical techniques (impedance spectroscopy and potentiodynamic polarisation). Inhibition efficiency increases with 2MBI concentration to attain 98% at 10^{-3} M. Polarisation curves indicate that 2MBI acts as a mixed-type inhibitor. Inhibition efficiency values obtained from various methods were in good agreement. EIS measurements showed an increase of the transfer resistance with the inhibitor concentration. The temperature effect on the corrosion behaviour of steel in 1.0 M HCl without and with the 2MBI at various concentrations was studied in the temperature range from 308 to 353 K. Thermodynamic parameters such as heat of adsorption ($\Delta H_{\text{ads}}^{\circ}$), entropy of adsorption ($\Delta S_{\text{ads}}^{\circ}$) and adsorption free energy ($\Delta G_{\text{ads}}^{\circ}$) have been calculated. Kinetic parameters for the corrosion reaction at different concentrations of 2MBI were determined. Adsorption of 2MBI on the mild steel surface in 1.0 M HCl follows the Langmuir isotherm model.

© 2010 King Saud University. All rights reserved.

* Corresponding author at: Electrochemistry Research Laboratory, Chemistry Department, Faculty of Education, Ain Shams University, Roxy, Cairo, Egypt.
E-mail address: khaledrice2003@yahoo.com (K.F. Khaled).

1878-5352 © 2010 King Saud University. All rights reserved. Peer-review under responsibility of King Saud University.
doi:10.1016/j.arabjc.2010.06.010



1. Introduction

Hydrochloric acid is a strong inorganic acid that is used in many industrial processes. The most important areas of applications are acid pickling, acid descaling and oil well acidizing. During these processes, metal such as steel is subjected to serious acid corrosion and inhibitors are often needed to reduce corrosion rates in this media.

Most of the efficient inhibitors used in industry are organic compounds having multiple bonds in their molecules, which mainly contain nitrogen and sulphur. Nitrogen-containing

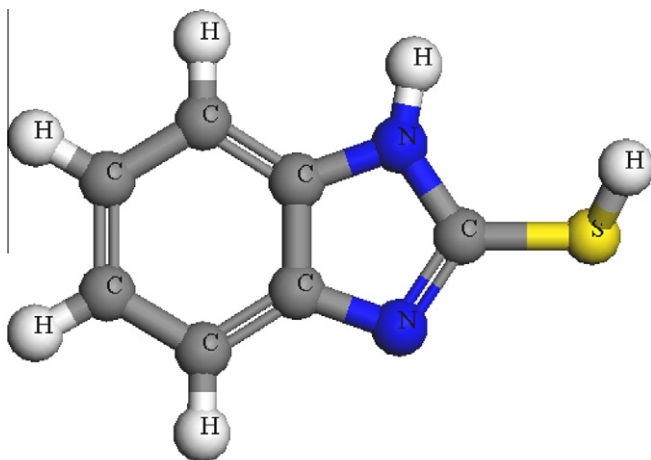
compounds are more effectively in HCl (Bentiss et al., 2000; Abd El-Maksoud, 2003), whereas sulphur-containing compounds are preferred for H₂SO₄. These compounds can adsorb on metal surface and block the cathodic and/or anodic sites on the metal surface which lead to decrease the corrosion rate (Fisher, 1972; Riggs Jr., 1974). The mode of adsorption depends mainly on the chemical structure of the inhibitor, the chemical composition of the solution, the nature of the metal surface and the electrochemical potential of the metal-solution interface (Ita and Offiong, 1997a,b; Lukovits et al., 2001).

A survey of literature shows that nitrogen-containing organic compounds, such as amines, heterocyclic compounds (Ousslim et al., 2009; Sykes, 1984; Tang et al., 2003; Mernari et al., 1998; Bentiss et al., 2000; Walker, 1975; Xue et al., 1991; Wang et al., 2002; Kertit and Hammouti, 1996) and imidazole derivatives (Stupnicek-Lisac et al., 2002; Sivaraju et al., 2008; Khaled and Amin, 2009; Zhang et al., 2004; Christov and Popova, 2004; Khaled, 2003) offer good protection of metallic materials in acidic solutions. The encouraging results obtained with 2-mercapto benzimidazole (Wang et al., 2003; Popova et al., 2003; Trachli et al., 2002; Wang, 2001; Aljourani et al., 2009; Amar et al., 2007; Khaled and Fadl-Allah, 2009) have incited us to extend its use in the corrosion-inhibiting action on mild steel in HCl solution.

The aim of this work is to study the effect of 2-mercapto benzimidazole (2MBI) on the corrosion inhibition of mild steel in molar hydrochloric acid solution. The behaviour of steel in 1.0 M HCl with and without inhibitor is studied using gravimetric, potentiodynamic and EIS measurements. The thermodynamic parameters for the adsorption process and activation parameters for steel dissolution reactions are determined and discussed.

2. Experimental

2-Mercapto benzimidazole (2MBI) was analytical grade. The molecular structure is shown below:



Chemical structure of 2-mercapto benzimidazole.

The aggressive solution (1.0 M HCl) was prepared by dilution of analytical grade 37% HCl solution with double-distilled water. Prior to all measurements, the steel samples with the following composition (0.09% P; 0.38% Si; 0.01% Al; 0.05%

Mn; 0.21% C; 0.05% S and the remainder iron) were abraded with different emery papers up to 1200 grade, washed thoroughly with double-distilled water, degreased with AR grade ethanol, acetone and drying at room temperature.

Gravimetric measurements were carried out in a double walled glass cell equipped with a thermostat-cooling condenser. The solution volume was 100 ml. The steel specimens used had a rectangular form (2.5 cm × 2 cm × 0.05 cm). The immersion time for the weight loss was 6 h at 308 K and 1 h at the other temperatures. After the corrosion test, the specimens of steel were carefully washed in double-distilled water, dried and then weighed. The rinse removed loose segments of the film of the corroded samples. Triplicate experiments were performed in each case and the mean value of the weight loss is reported. Weight loss allowed us to calculate the mean corrosion rate as expressed in mg cm⁻² h⁻¹.

Electrochemical measurements were carried out in a conventional three-electrode electrolysis cylindrical Pyrex glass cell. The working electrode (WE) in the form of disc cut from steel has a geometric area of 1 cm² and is embedded in polytetrafluoroethylene (PTFE). A saturated calomel electrode (SCE) and a disc platinum electrode were used as reference and auxiliary electrodes, respectively. The temperature was thermostatically controlled at 308 ± 1 K. The working electrode, WE was abraded with silicon carbide paper (grade P1200), degreased with acetone and rinsed with double-distilled water before use.

Running on a personal computer, the 352 Soft Corr™ III software communicates with EG&G Instruments potentiostat-galvanostat model 263 A at a scan rate of 0.5 mV s⁻¹. Before recording the cathodic polarisation curves, the steel electrode is polarised at -800 mV for 10 min. For anodic curves, the potential of the electrode is swept from its corrosion potential after 30 min at free corrosion potential, to more positive values. The test solution is deaerated with pure nitrogen. Gas bubbling is maintained through the experiments.

The electrochemical impedance spectroscopy (EIS) measurements were carried out with the electrochemical system (Tacussel) which included a digital potentiostat model Voltalab PGZ 100 computer at E_{corr} after immersion in solution without bubbling, the circular surface of steel exposing of 1 cm² to the solution were used as working electrode. After the determination of steady-state current at a given potential, sine wave voltage (10 mV) peak to peak, at frequencies between 100 kHz and 10 mHz were superimposed on the rest potential. Computer programs automatically controlled the measurements performed at rest potentials after 30 min of exposure. The impedance diagrams are given in the Nyquist representation. Values of R_t and C_{dl} were obtained from Nyquist plots.

3. Results and discussion

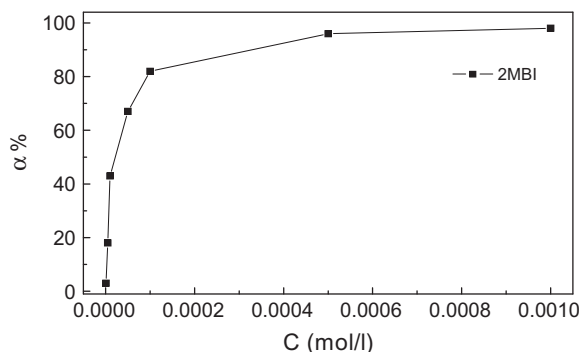
3.1. Weight loss tests

Gravimetric measurements of steel were investigated in 1.0 M HCl in the absence and presence of various 2MBI concentrations at 6 h of immersion and at 308 K. The inhibition efficiency ($\alpha\%$) was calculated by the following relation:

$$\alpha\% = \frac{W_{\text{corr}} - W_{\text{corr(inh)}}}{W_{\text{corr}}} \times 100 \quad (1)$$

Table 1 Gravimetric results of mild steel in 1.0 M HCl without and with addition of 2MBI.

Concentration ($\times 10^3$ M)	W ($\text{mg cm}^{-2} \text{h}^{-1}$)	$\alpha\%$
0.000	1.151	–
0.001	1.113	03
0.005	0.943	18
0.010	0.661	43
0.050	0.374	67
0.100	0.203	82
0.500	0.041	96
1.000	0.026	98

**Figure 1** Variation of inhibition efficiency ($\alpha\%$) with the concentration of 2MBI for mild steel in 1.0 M HCl.

where W_{corr} and $W_{\text{corr (inh)}}$ are the corrosion rates of steel in the absence and presence of the organic compound, respectively.

Table 1 collects the corrosion rates and Fig. 1 shows the variation of inhibition efficiencies evaluated from weight loss measurements for different inhibitor concentrations in 1.0 M HCl. The corrosion rate decreases with 2MBI concentration and in turn the inhibition efficiency ($\alpha\%$) increases to attain 98%. From weight loss measurements, we can conclude that 2MBI is an excellent inhibitor.

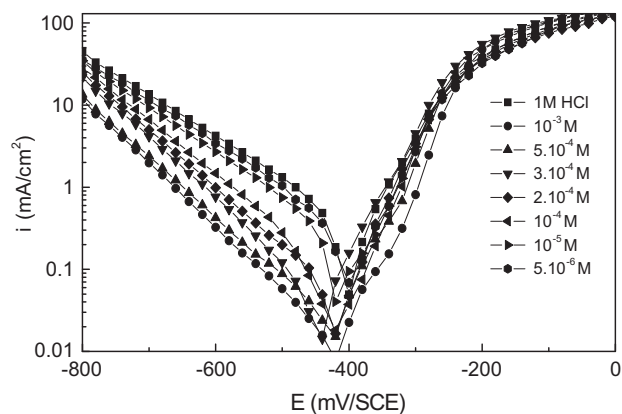
3.2. Polarisation measurements

The polarisation curves of steel recorded in 1.0 M HCl in the absence and presence of 2MBI at different concentration at 308 K are presented in Fig. 2. The extrapolation method for the polarisation curves was applied and the data for corrosion potential (E_{corr}), corrosion current density (I_{corr}), cathodic Tafel slopes (b_c) and percentage inhibition efficiency ($\eta\%$) are shown in Table 2. The relation determines the inhibition efficiency ($\eta\%$):

$$\eta\% = \frac{I_{\text{corr}} - I_{\text{corr(inh)}}}{I_{\text{corr}}} \times 100 \quad (2)$$

where I_{corr} and $I_{\text{corr (inh)}}$ are the corrosion current density values without and with the inhibitor, respectively, determined by extrapolation of cathodic Tafel lines to the corrosion potential.

As it is shown in Fig. 2 and Table 2, cathodic current–potential curves give rise to parallel Tafel lines indicating that the hydrogen evolution reaction is under activation controlled. The cathodic current density decreases with the concentration of 2MBI however, a slight effect is observed on the anodic por-

**Figure 2** Potentiodynamic curves for mild steel in 1.0 M HCl in the presence of various 2MBI concentrations.**Table 2** Electrochemical parameters of mild steel at various concentrations of 2MBI in 1.0 M HCl and corresponding inhibition efficiencies.

Concentration ($\times 10^3$ M)	E_{corr} (mV)	b_c (mV dec^{-1})	I_{corr} ($\mu\text{A cm}^{-2}$)	$\eta\%$
0.000	–418	188	508	–
0.001	–424	185	428	16
0.005	–420	178	286	44
0.010	–422	153	103	80
0.050	–429	145	65	87
0.100	–435	139	42	92
0.500	–434	137	23	96
1.000	–432	130	17	97

tions. This result indicates that 2MBI is adsorbed on the metal surface on the cathodic sites and hence inhibition occurs.

These results demonstrate that the hydrogen reduction is inhibited and that the inhibition efficiency increases with inhibitor concentration to attain 97 at 10^{-3} M of 2MBI.

We remark that the inhibitor acts on the anodic portion and the anodic current density is reduced (Fig. 2). It seems also that the presence of the inhibitor change slightly the corrosion potential values in no definite direction. These results indicated that 2MBI acts as a mixed-type inhibitor.

3.3. Effect of 2MBI concentration on the corrosion rate of steel at various temperatures

The effect of temperature on the anti-corrosion effectiveness of 2MBI, was studied at various 2MBI concentrations in the temperature domain (313–353 K) after 1 h of immersion. The collected curves in Fig. 3 show the evolution of corrosion rate (W) with 2MBI concentration (C) at different temperatures.

Fig. 3 indicates that at a given 2MBI concentration the corrosion rate of steel increased with temperature. The increase is more pronounced at low concentrations. The results also indicate that for a given temperature, the corrosion rate of steel decreased with increasing inhibitor concentration. The values of inhibition efficiency obtained from the weight loss for different inhibitor concentrations and at various temperatures in 1.0 M HCl are given in Table 3 and Fig. 4. It is clear that inhibition efficiency increased with increase in inhibitor concentration.

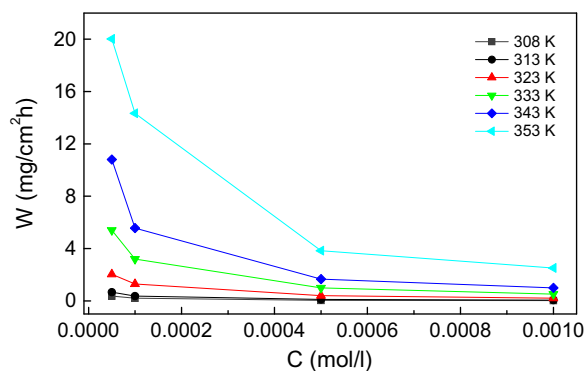


Figure 3 Variation of corrosion rate with the concentrations of 2MBI for mild steel in 1.0 M HCl at different temperatures.

Table 3 Weight loss data and inhibition efficiencies obtained at different concentrations of 2MBI and different temperatures at 1 h.

Temperature (K)	Concentration ($\times 10^3$ M)	W (mg cm ⁻² h ⁻¹)	$\alpha\%$	θ
313	0.000	1.431	–	–
	0.050	0.667	53	0.53
	0.100	0.367	74	0.74
	0.500	0.111	92	0.92
	1.000	0.046	97	0.97
323	0.000	3.134	–	–
	0.050	2.035	35	0.35
	0.100	1.295	59	0.59
	0.500	0.392	87	0.87
	1.000	0.208	93	0.93
333	0.000	6.618	–	–
	0.050	5.402	18	0.18
	0.100	3.202	52	0.52
	0.500	0.995	85	0.85
	1.000	0.521	92	0.92
343	0.000	11.37	–	–
	0.050	10.801	05	0.05
	0.100	5.57	51	0.51
	0.500	1.672	85	0.85
	1.000	0.989	91	0.91
353	0.000	20.45	–	–
	0.050	20.02	02	0.02
	0.100	14.34	30	0.3
	0.500	3.84	81	0.81
	1.000	2.513	88	0.88

The maximum value of inhibition efficiency ($\alpha\%$) obtained for 10^{-3} M 2MBI is 98% at 308 K.

The inhibition efficiencies decrease slightly with increasing temperature indicating that higher temperature dissolution of steel predominates on adsorption of 2MBI at the metal surface.

3.4. Apparent activation energy (E_a) and pre-exponential factor (A)

In order to obtain more details on the corrosion process, activation kinetic parameters such energy (E_a), enthalpy (ΔH_a°)

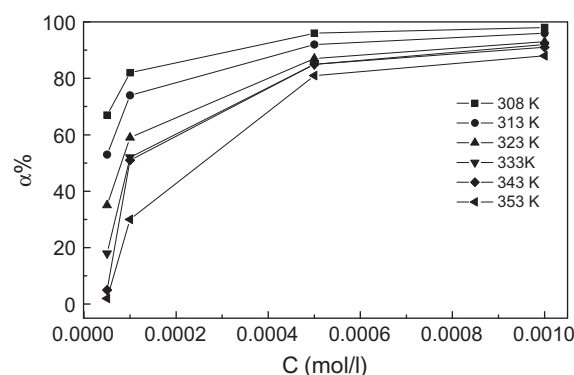


Figure 4 Variation of inhibition efficiency ($\alpha\%$) with concentration of 2MBI for mild steel in 1.0 M HCl at different temperatures.

and entropy (ΔS_a°) evaluated from the effect of temperature using Arrhenius law (Eq. (3)) and the alternative formulation of Arrhenius equation (Eq. (4)) (Aljourani et al., 2009):

$$W = A \exp\left(-\frac{E_a}{RT}\right) \quad (3)$$

$$W = \frac{RT}{Nh} \exp\left(\frac{\Delta S_a^\circ}{R}\right) \exp\left(-\frac{\Delta H_a^\circ}{RT}\right) \quad (4)$$

where W is the corrosion rate, R is the universal gas constant, T is the absolute temperature, A is the pre-exponential factor, h is Plank's constant and N is Avogadro's number.

Fig. 5 shows Arrhenius plot of the corrosion rate for mild steel in 1.0 M HCl in the presence of different concentrations of 2MBI. Straight lines are obtained. The activation energies are estimated from the slopes ($-E_a/R$). Additionally The straight lines obtained from the transition state plot of the corrosion rate for mild steel in 1.0 M HCl in the presence of different concentrations of 2MBI (Fig. 6) permit the calculation of ΔH_a° and ΔS_a° , respectively, from slopes ($-\Delta H_a^\circ/R$) and intercepts ($\ln R/Nh + \Delta S_a^\circ/R$). E_a , ΔH_a° and ΔS_a° are collected in Table 4.

Previous studies (Aljourani et al., 2009; Elachouri et al., 1996; Ferreira et al., 2004) showed that compared with the activation energy in the absence of inhibitor, higher values

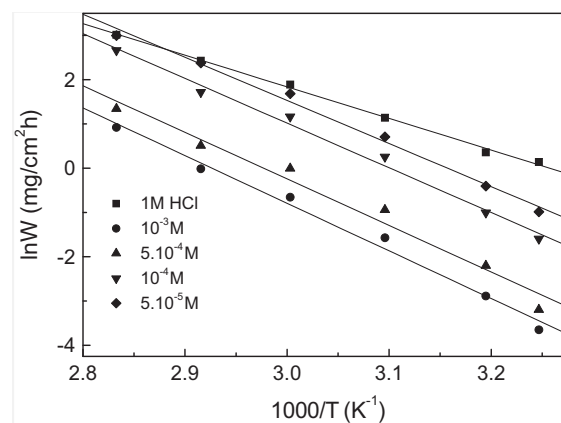


Figure 5 Arrhenius plot of the corrosion rate for mild steel in 1.0 M HCl in the presence of different concentrations of 2MBI.

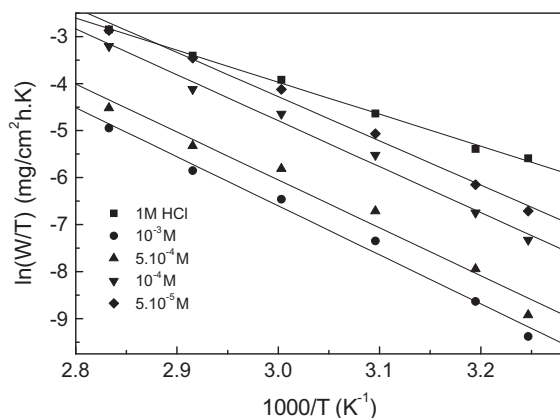


Figure 6 Transition state plot of the corrosion rate for mild steel in 1.0 M HCl in the presence of different concentrations of 2MBI.

for E_a were found in the presence of inhibitor. Other studies (Banerjee and Misra, 1989; Ferreira et al., 2004) showed that in the presence of 2MBI, the activation energy was lower than that in its absence.

It was clear that (see Table 4) the values of E_a in the presence of the 2MBI are higher than that in the uninhibited acid solution (59.39 kJ mol⁻¹).

The decrease of inhibition efficiencies with increasing temperature and the increase of E_a in the presence of the inhibitor indicate the physical adsorption mechanism (Popova et al., 2003).

Fig. 7 indicates that the activation energy increases with the concentration of 2MBI. In the same way, the pre-exponential factor increases with the concentration of 2MBI (as shown in Table 4). The pre-exponential factor and activation energy varies in the same way. From Eq. (3), it can be seen that at a certain temperature, the value of the steel corrosion rate is jointly decided by the apparent activation energy and pre-exponential factor. As a whole, the steel corrosion rate basically decreases with an increase in concentration of 2MBI. As can be seen from Table 4, it was clear that both E_a and A increased in the presence of 2MBI (Mu et al., 2004).

The variation of activation parameters E_a and ΔH_a° with 2MBI concentration is shown in Fig. 7. From the data obtained in Table 4, it seems that E_a increases with the inhibitor concentration. The positive sign of the enthalpy (ΔH_a°) reflects the endothermic nature of the steel dissolution process (Table 4). We remark that E_a and ΔS_a° values vary in the same way with the inhibitor concentration. This result permit to verify the known thermodynamic relation (Gomma and Wahdan, 1995) between E_a and ΔS_a° as shown also in Table 4:

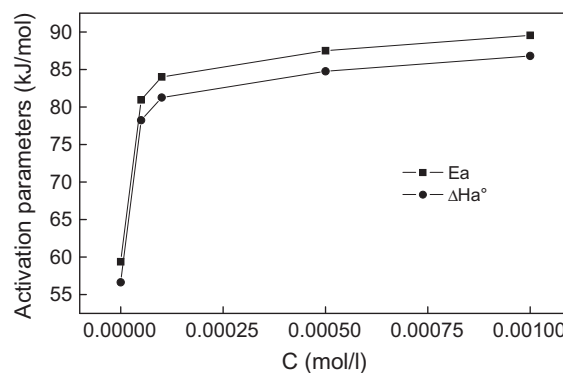


Figure 7 Variation of activation parameters E_a and ΔH_a° with 2MBI concentration for mild steel in 1.0 M HCl.

$$E_a - \Delta H_a^\circ = RT \quad (5)$$

The calculated values are very close to RT which is equal 2.67 kJ mol⁻¹ at 323 K.

The positive values of entropies (ΔS_a°) in the presence of inhibitor imply that the activated complex in the rate determining step represents an association rather than a dissociation step, meaning that an increase in disordering takes place on going from reactants to the activated complex (Elachouri et al., 1996).

3.5. Adsorption isotherm and thermodynamic parameters

Assuming the corrosion inhibition was caused by the adsorption of 2MBI, and the values of surface coverage (θ) for different concentrations of 2MBI in 1 M HCl were evaluated from weight loss measurements using the Sekine and Hirakawa's method (Sekine and Hirakawa, 1986):

$$\theta = \frac{W_0 - W}{W_0 - W_m} \quad (6)$$

where W_m is the smallest corrosion rate.

In order to get a better understanding of the electrochemical process on the metal surface, adsorption characteristics are also studied for 2MBI. This process is closely related to the adsorption of the inhibitor molecules (Hackerman and Sudbury, 1950; Hackerman, 1962) and adsorption is known to depend on the chemical structure (Cheng et al., 1999; Ateya et al., 1984; Akiyama and Nobe, 1970). Adsorption isotherms are very important in determining the mechanism of organic electrochemical reactions. The most frequently used adsorption isotherms are Langmuir, Temkin and Frumkin.

In hydrochloric acid solution, the organic compound follows the Langmuir adsorption isotherm. This is as follows:

Table 4 Some activation parameters as function of 2MBI concentration.

Concentration ($\times 10^3$ M)	Pre-exponential factor (kg m ⁻² s ⁻¹)	Linear regression coefficient	E_a (kJ mol ⁻¹)	ΔH_a° (kJ mol ⁻¹)	ΔS_a° (J mol ⁻¹ K ⁻¹)	$E_a - \Delta H_a^\circ$ (kJ mol ⁻¹)
0.000	3.50×10^{10}	0.998	59.39	56.65	-60.75	2.64
0.050	6.14×10^{13}	0.997	80.96	78.23	1.41	2.73
0.010	1.10×10^{14}	0.996	84.01	81.27	6.53	2.74
0.500	1.10×10^{14}	0.997	87.49	84.75	6.26	2.74
1.000	1.33×10^{14}	0.995	89.54	86.81	7.81	2.73

Table 5 Adsorption parameters of the linear regression between C/θ and C of 2MBI.

Temperature (K)	Linear regression coefficient	K	Slope	$\Delta G_{\text{ads}}^{\circ}$ (kJ mol ⁻¹)	$\Delta H_{\text{ads}}^{\circ}$ (kJ mol ⁻¹)	$\Delta S_{\text{ads}}^{\circ}$ (J mol ⁻¹ K ⁻¹)
308	1.0000	45537.8	0.998	-37.78	-36.26	4.93
313	0.9999	27426.9	1.007	-37.07	-36.26	2.59
323	0.9999	14316.4	1.006	-36.51	-36.26	0.77
333	1.0000	10838.5	0.994	-36.87	-36.26	1.83
343	0.9999	10830.2	1.004	-37.97	-36.26	4.99
353	0.9899	4616.8	0.899	-36.58	-36.26	0.91

$$\frac{\theta}{1-\theta} = KC \quad (7)$$

Rearranging this equation gives:

$$\frac{C}{\theta} = \frac{1}{K} + C \quad (8)$$

where C is the concentration of inhibitor, K is the equilibrium constant of the adsorption process, and θ is the surface coverage.

From the values of surface coverage, the linear regressions between C/θ and C are calculated and the parameters (adsorption coefficients, slopes, and linear regression coefficients) are listed in Table 5. Fig. 8 shows the relationship between C/θ and C at various temperatures. These results show that the linear regression coefficients (r) and the slopes are almost equal 1.000, indicating that the adsorption of inhibitor onto steel surface agrees the Langmuir adsorption isotherm.

In addition, the equilibrium constant of the adsorption process (K) decreases with increasing temperature (Table 5). It is well known that K designates the adsorption power of inhibitor onto the steel surface; clearly, 2MBI gives higher values of K at lower temperatures, indicating that it was adsorbed strongly onto the steel surface. Thus, the inhibition efficiency decreased slightly with the increase in temperature as the result of the improvement for the desorption of 2MBI from the steel surface.

The corrosion inhibition of 2MBI for steel may be well explained by using thermodynamic model, so, the heat, the free energy and the entropy of adsorption are calculated to elucidate the phenomenon for the inhibition action of 2MBI.

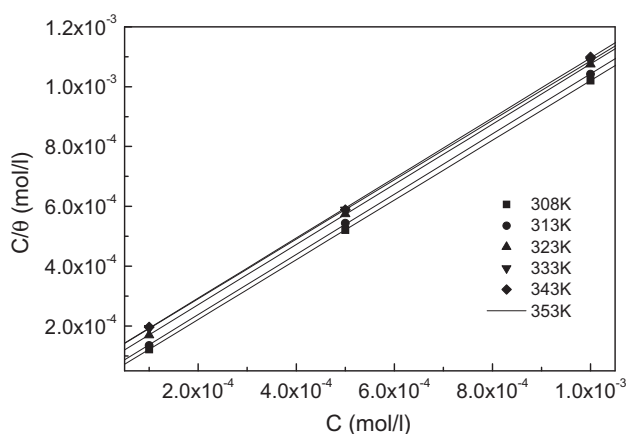


Figure 8 Curve fitting of the corrosion data for mild steel in 1.0 M HCl in the presence of different concentrations of 2MBI to the Langmuir isotherm at different temperatures.

According to the Van't Hoff equation (Tang et al., 2003; Zhao and Mu, 1999):

$$\ln(K) = -\frac{\Delta H_{\text{ads}}^{\circ}}{RT} + \text{Constant} \quad (9)$$

where $\Delta H_{\text{ads}}^{\circ}$ and K are the adsorption heat and adsorptive equilibrium constant, respectively.

To obtain the adsorption heat, the linear regression between $\ln K$ and $1/T$ is dealt with, the relationship between $\ln K$ and $1/T$ is shown in Fig. 9. Under the experimental conditions, the adsorption heat could be approximately regarded as the standard adsorption heat ($\Delta H_{\text{ads}}^{\circ}$) (Mu et al., 2004; Zhao and Mu, 1999). The obtained value of $\Delta H_{\text{ads}}^{\circ}$ is -36.26 kJ mol⁻¹. The standard adsorption free energy ($\Delta G_{\text{ads}}^{\circ}$) is obtained according to the following equation (Khamis, 1990):

$$K = \frac{1}{55.5} \exp\left(-\frac{\Delta G^{\circ}}{RT}\right) \quad (10)$$

The negative values of $\Delta G_{\text{ads}}^{\circ}$ (Table 5) ensure the spontaneity of the adsorption process and stability of the adsorbed layer on the steel surface (Ali et al., 2005). Furthermore, it is found that $\Delta G_{\text{ads}}^{\circ}$ slightly increases with temperature.

The negative values of $\Delta H_{\text{ads}}^{\circ}$ also show that the adsorption of inhibitor is an exothermic process (Gomma and Wahdan, 1995). Generally, an exothermic process signifies either physisorption or chemisorption while endothermic process is attributable unequivocally to chemisorption (Durnie et al., 1999). In an exothermic process, physisorption is distinguished from chemisorption by considering the absolute value of a physisorption process is lower than 40 kJ mol⁻¹ while the adsorption heat

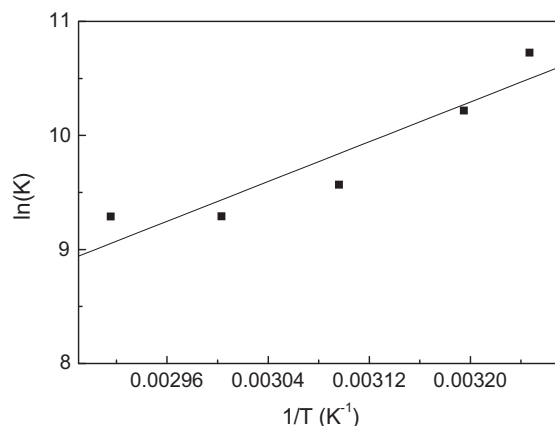


Figure 9 Variation of $\ln(K)$ with $1/T$ for mild steel in 1.0 M HCl in the presence of 2MBI.

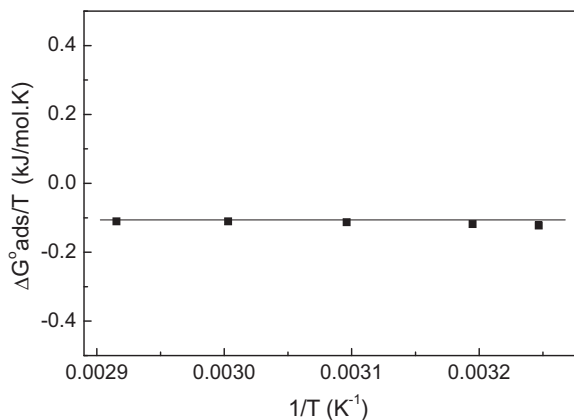


Figure 10 Variation of $\Delta G_{\text{ads}}^{\circ}/T$ with $1/T$ for mild steel in 1.0 M HCl in the presence of 2MBI.

of a chemisorption process approaches 100 kJ mol^{-1} (Martinez and Stern, 2002). In the present case; the standard adsorption heat $-36.26 \text{ kJ mol}^{-1}$ shows that a comprehensive adsorption (physical adsorption) might occur (Tang et al., 2003). The same results were obtained in previous studies (Trachli et al., 2002; Li and Mu, 2005). The adsorption of inhibitor molecules is accompanied by positive values of $\Delta S_{\text{ads}}^{\circ}$.

$\Delta H_{\text{ads}}^{\circ} = -36.26 \text{ kJ mol}^{-1}$ found by the Van't Hoff equation, may be also evaluated by the Gibbs–Helmholtz equation, which is defined as follows:

$$\left[\frac{\partial(\Delta G_{\text{ads}}^{\circ}/T)}{\partial T} \right]_{\text{p}} = -\frac{\Delta H_{\text{ads}}^{\circ}}{T^2} \quad (11)$$

which can be arranged to give the following equation:

$$\frac{\Delta G_{\text{ads}}^{\circ}}{T} = \frac{\Delta H_{\text{ads}}^{\circ}}{T} + A \quad (12)$$

The variation of $\Delta G_{\text{ads}}^{\circ}/T$ with $1/T$ gives a straight line with a slope that equals $\Delta H_{\text{ads}}^{\circ}$ (Fig. 10). It can be seen from Fig. 10 that $\Delta G_{\text{ads}}^{\circ}/T$ decreases slightly with $1/T$ in a linear fashion. The values of $\Delta H_{\text{ads}}^{\circ}$ is negative ($\Delta H_{\text{ads}}^{\circ} = -36.26 \text{ kJ mol}^{-1}$), reflecting the exothermic behaviour of adsorption on the steel surface.

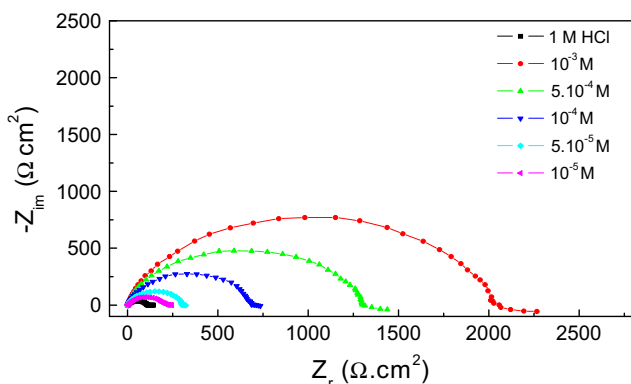


Figure 11 Nyquist diagrams for steel in 1.0 M HCl in the presence of different of 2MBI concentrations.

The value of the enthalpy of adsorption found by the two methods such as Van't Hoff and Gibbs–Helmholtz relations are in good agreement.

3.6. Electrochemical impedance spectroscopy (EIS)

Fig. 11 shows a typical set of Nyquist plots for mild steel in 1.0 M HCl in the absence and presence of various concentrations of 2-mercapto benzimidazole. It is clear from these plots that the impedance response of mild steel has significantly changed after the addition of 2MBI in 1.0 M HCl. The impedance parameters derived from these plots using equivalent circuit described elsewhere (Khaled, 2003) are given in Table 6.

The charge transfer resistance, R_t values are calculated from the difference in impedance at lower and higher frequencies, as suggested by Tsuru and Haruyama (Mansfeld et al., 1981a,b; Tsuru et al., 1978). To obtain the double capacitance (C_{dl}), the frequency at which the imaginary component of the impedance is maximum ($-Z_{\text{max}}$) is found and C_{dl} values are obtained from the equation:

$$f(-Z_{\text{max}}) = \frac{1}{2\pi C_{\text{dl}} R_t} \quad (13)$$

The charge transfer resistance (R_{ct}), double layer capacitance (C_{dl}) and inhibition efficiency $\chi\%$

$$\chi\% = \frac{R_{\text{tcorr}}^{-1} - R_{\text{tcorr(inh)}}^{-1}}{R_{\text{tcorr}}^{-1}} \times 100 \quad (14)$$

where R_{tcorr} and $R_{\text{tcorr(inh)}}$ are the charge transfer resistance values without and with inhibitor, respectively.

Table 6 indicates that by increasing the concentration of 2MBI, the C_{dl} values tended to decrease and the inhibition efficiency improved. This decrease in the C_{dl} , which can result from a decrease in local dielectric constant and/or an increase in the thickness of the electrical double layer, signifying that 2MBI molecules act by adsorption at the metal/solution interface (McCafferty and Hackerman, 1972).

The double layer capacitance C_{dl} is expressed in the Helmutz model by:

$$C_{\text{dl}} = \frac{\epsilon_0 \epsilon}{\delta} S \quad (15)$$

where δ is the thickness of the deposit, S is the surface area of the working electrode, ϵ_0 is the permittivity of the air and ϵ is the medium dielectric constant.

The decrease in C_{dl} values may be interpreted either by a decrease of local dielectric constant ϵ (McCafferty and

Table 6 Characteristic parameters evaluated from the impedance diagram for steel in 1.0 M HCl at various concentrations of 2MBI.

2MBI concentration (M)	R_t ($\Omega \text{ cm}^2$)	f_{max} (Hz)	C_{dl} ($\mu\text{F cm}^{-2}$)	$\chi\%$
0	106.9	15.82	94.1	
10^{-6}	112.5	17.86	79.2	5
10^{-5}	196.5	10.01	81.1	46
5×10^{-5}	307.6	6.79	76.2	65
10^{-4}	699.1	3.57	63.7	85
5×10^{-4}	1302.1	2.23	54.8	92
10^{-3}	2026.7	1.58	49.7	95

Hackerman, 1972) or by the thickness of the adsorbate layer of inhibitor at the metal surface (Bastidas et al., 2000).

The data obtained from EIS are in good harmony with that obtained from potentiodynamic polarisation. The impedance spectra obtained on mild steel in 1.0 M HCl solutions consist of one depressed capacitive loop (one time constant in the Bode-phase representation, not shown here). When Nyquist plot contains a “depressed semicircle with the center under the real axis”, such behaviour is characteristic for solid electrodes and often referred to as frequency dispersion that has been attributed to roughness and other inhomogeneities of the solid surface (Khaled, 2003).

Deviation of this kind often referred to as frequency dispersion. Therefore, a constant phase element (CPE) instead of a capacitive element is used in Fig. 2 to get a more accurate fit of experimental data sets using generally more complicated equivalent circuits. The impedance, Z , of CPE has the form (Khaled, 2003):

$$Z_{\text{CPE}} = [Q(j\omega)^n]^{-1} \quad (16)$$

where Q is the CPE constant, which is a combination of properties related to the surface and electro-active species, $j^2 = -1$ the imaginary number, ω the angular frequency and n is a CPE exponent which can be used as a measure of the heterogeneity or roughness of the surface. Depending on the value of n , CPE can represent resistance ($n = 0$, $Q = 1/R$), capacitance ($n = 1$, $Q = C$), inductance ($n = -1$, $Q = 1/L$) or Warburg impedance ($n = 0.5$, $Q = W$) Khaled, 2003.

4. Conclusions

From the above results and discussion, the following conclusions are drawn:

- 2MBI inhibits the corrosion of steel in 1.0 M HCl. The inhibition efficiency increases with the inhibitor concentration, but decrease slightly with the temperature.
- 2MBI acts as a mixed-type inhibitor.
- The adsorption of 2MBI on the steel surface from 1.0 M HCl obeys a Langmuir adsorption isotherm. The adsorption process is a spontaneous and exothermic process.
- The kinetic and thermodynamic parameters of corrosion and adsorption processes are determined.
- The results obtained from weight loss, potentiodynamic polarisation and impedance spectroscopy are in good agreement.

References

Abd El-Maksoud, S.A., 2003. Appl. Surf. Sci. 206, 129.
 Akiyama, A., Nobe, K., 1970. J. Electrochem. Soc. 17, 999.
 Ali, S.A., El-Shareef, A.M., Al-Ghamdi, R.F., Saeed, M.T., 2005. Corros. Sci. 47, 2659.
 Aljourani, J., Raeissi, K., Golozara, M.A., 2009. Corros. Sci. 51, 1836.
 Amar, H., Tounsi, A., Makayssi, A., Derja, A., Benzakour, J., Outzourhit, A., 2007. Corros. Sci. 49, 2936.

Ateya, B.G., El-Anadouli, B.E., El-Nizamy, F.M., 1984. Corros. Sci. 24, 509.
 Banerjee, S.N., Misra, S., 1989. Corrosion 45, 780.
 Bastidas, J.M., Polo, J.L., Cano, E., 2000. J. Appl. Electrochem. 30, 1173.
 Bentiss, F., Traisnel, M., Lagrenée, M., 2000. Corros. Sci. 42, 127.
 Cheng, X.L., Ma, H.Y., Chen, S.H., Yu, R., Chen, X., Yao, Z.M., 1999. Corros. Sci. 41, 321.
 Christov, M., Popova, A., 2004. Corros. Sci. 46, 1613.
 Durnie, W., De Marco, R., Kinsella, B., Jefferson, A., 1999. J. Electrochem. Soc. 146, 1751.
 Elachouri, M., Hajji, M.S., Salem, M., Kertit, S., Aride, J., Coudert, R., Essassi, E., 1996. Corrosion 52, 103.
 Ferreira, E.S., Giacomelli, C., Giacomelli, F.C., Spinelli, A., 2004. Mater. Chem. Phys. 83, 129.
 Fisher, H., 1972. Werks. Korros. 23, 253.
 Gomma, G.K., Wahdan, M.H., 1995. Mater. Chem. Phys. 39, 211.
 Hackerman, N., 1962. Corrosion 18, 332.
 Hackerman, N., Sudbury, J.D., 1950. J. Electrochem. Soc. 94, 4.
 Ita, B.I., Offiong, O.E., 1997a. Mater. Chem. Phys. 51, 203.
 Ita, B.I., Offiong, O.E., 1997b. Mater. Chem. Phys. 48, 164.
 Kertit, S., Hammouti, B., 1996. Appl. Surf. Sci. 93, 59.
 Khaled, K.F., 2003. Electrochim. Acta 48, 2493.
 Khaled, K.F., Amin, M.A., 2009. J. Appl. Electrochem. 39, 429.
 Khaled, K.F., Fadl-Allah, S.A., 2009. Mater. Chem. Phys. 117, 148.
 Khamis, E., 1990. Corrosion 46, 476.
 Li, X., Mu, G., 2005. Appl. Surf. Sci. 252, 1254.
 Lukovits, I., Kalman, E., Zucchi, F., 2001. Corrosion (Houston) 57 (1), 3.
 Mansfeld, F., Kending, M.W., Tsai, S., 1981a. Corrosion 37, 301.
 Mansfeld, F., Kending, M.W., Tsai, S., 1981b. Corrosion 38, 570.
 Martinez, S., Stern, I., 2002. Appl. Surf. Sci. 199, 83.
 McCafferty, E., Hackerman, N., 1972. J. Electrochem. Soc. 119, 146.
 Mernari, B., Elattari, H., Traisnel, M., Bentiss, F., Lagrenée, M., 1998. Corros. Sci. 40, 391.
 Mu, G.N., Li, X.M., Li, F., 2004. Mater. Chem. Phys. 86, 59.
 Ousslim, A., Bekkouch, K., Hammouti, B., Elidriissi, A., Aouiti, A., 2009. J. Appl. Electrochem. 39, 1075.
 Popova, A., Sokolova, E., Raicheva, S., Christov, M., 2003. Corros. Sci. 45, 33.
 Riggs Jr., O.L., 1974. in: Nathan, C.C. (Ed.), Corrosion Inhibitors, second ed. NACE, Houston, TX.
 Sekine, I., Hirakawa, Y., 1986. Corrosion 42, 272.
 Sivaraju, M., Kannan, K., Elavarasan, S., 2008. Orient. J. Chem. 25, 67.
 Stupnicek-Lisac, E., Gazivoda, A., Madzarac, M., 2002. Electrochim. Acta 47, 4189.
 Sykes, J.M., 1984. Br. Corros. J. 25, 175.
 Tang, L.B., Mu, G.N., Liu, G.H., 2003. Corros. Sci. 45, 2251.
 Trachli, B., Keddad, M., Takenouti, H., Srhiri, A., 2002. Prog. Org. Coat. 44, 17.
 Tsuru, T., Haruyama, S., Gijitsu, B., 1978. J. Jpn. Soc. Corros. Eng. 27, 573.
 Walker, R., 1975. Corros. Sci. 31, 97.
 Wang, L., 2001. Corros. Sci. 43, 2281.
 Wang, H.L., Fan, H.B., Zheng, J.S., 2002. Mater. Chem. Phys. 77, 655.
 Wang, L., Pu, J.X., Luo, H.C., 2003. Corros. Sci. 45, 677.
 Xue, G., Ding, J., Lu, P., Dong, J., 1991. J. Phys. Chem. 95, 7380.
 Zhang, D.Q., Gao, L.X., Zhou, G.D., 2004. Corros. Sci. 46, 3031.
 Zhao, T.P., Mu, G.N., 1999. Corros. Sci. 41, 1937.